Available online at www.sciencedirect.com
ScienceDirect
Journal of Organometallic Chemistry 692 (2007) 2299–2305
Journal of Organometallic Chemistry
www.elsevier.com/locate/jorganchem

Photoelectron spectroscopy of metal β-diketonato complexes

Igor Novak [a,*], Branka Kovač [b]

[a] Charles Sturt University, P.O. Box 883, Orange NSW 2800, Australia
[b] Physical Chemistry Division, "R. Bošković" Institute, HR-10002 Zagreb, Croatia

Received 17 October 2006; received in revised form 2 January 2007; accepted 31 January 2007
Available online 20 February 2007

Abstract

The electronic structures of yttrium(III), gadolinium(III) and ytterbium(III) tris-2,2,6,6-tetramethyl-3,5-heptanedione (tmhd) complexes have been investigated by HeI and HeII photoelectron spectroscopy (UPS), UDFT and OVGF calculations. We discuss metal–ligand bonding in the series of metal β-diketonato complexes on the basis of empirical arguments. The photoionization cross-sections and orbital energies of metal atoms must both be taken into account in order to rationalize changes in relative band intensities of the HeI/HeII spectra.

Keywords: Photoelectron spectroscopy; Metal diketonates

1. Introduction

Coordination complexes between metals and organic chelating ligands (e.g. acetylacetone; acac) are interesting because they provide models for chemical processes like adsorptions on the surfaces of metal catalysts or for bioinorganic molecules like metalloenzymes. The complexes between metals and acetylacetone derivatives were investigated by UV photoelectron spectroscopy (UPS) and quantum chemical calculations [1–5]. The UPS spectra of complexes between metals (e.g. Al^{3+}, Mg^{2+}, Ni^{2+}, V^{3+}, Cr^{3+}, Cu^{2+}, Zn^{2+}, Ga^{3+}, In^{3+}, Pd^{2+}, Pt^{2+}, rare-earths) and acac type ligands have complex appearances due to the high density of ionic states. The main interest in these studies was the nature of metal–ligand bonding and in particular the identification of orbitals with metal character. Quantum chemical calculations were used to analyze bonding, but due to the sizes of molecules the computational results were of limited accuracy. The use of CI method was recommended for the interpretation of UPS spectra [6] especially in view of the large reorganization effects taking place upon ionization [4c]. The magnetic moment measurements of rare-earth tmhd complexes (in solution/solid using NMR or Gouy balance) have indicated that Gd and Yb complexes are paramagnetic and have open shell electron configurations in the ground state [7]. Paramagneticity, together with large molecular size increases computational demands, increases the density of ionic states present (and hence spectral bandwidth) and reduces the reliability of calculated results [3,4a,4b]. Additional experimental information therefore becomes essential in order to get reliable understanding of metal–ligand bonding. This information may be obtained when UPS spectra are measured at several photon energies [3,4a,4c], because the changes in relative band intensities provide reliable insight into the nature of valence orbital ionizations. The reported UPS studies of rare-earth β-diketonato complexes [5b,8] suggested only a weak involvement of metal 4f orbitals in bonding. However, poor spectral resolution and absence of studies at variable photon energies make the suggestion tentative. The UPS study of β-diketonato transition metal complexes e.g. $Co(acac)_3$, $V(acac)_3$ and $Cr(acac)_3$ showed pronounced changes in HeI and HeII relative band intensities [3]. Each complex shows different HeI/HeII intensity changes which were (incompletely) rationalized by claiming

* Corresponding author.
E-mail address: inovak@csu.edu.au (I. Novak).

0022-328X/$ - see front matter © 2007 Elsevier B.V. All rights reserved.
doi:10.1016/j.jorganchem.2007.01.061

that this was due to certain orbitals in the complex having metal 3d character. We decided to reinvestigate the UPS work on metal β-diketonato complexes and provide a uniform explanatory framework regarding metal–ligand bonding and concomitant intensity changes.

We use experimentally derived metal orbital energies and calculated atomic orbital photoionization cross-sections in order to interpret the spectra and deduce the properties of metal–ligand bonding. The combined effect of these two factors on the spectral band intensities has not been considered previously.

2. Experimental and computational methods

The sample compounds: $Y(tmhd)_3$, $Gd(tmhd)_3$ and $Yb(tmhd)_3$ whose structural formulas are shown in Scheme 1, were purchased from Acros Organics and used without further purification after checking their identity and purity by MS and CH analysis.

The HeI/HeII photoelectron spectra were recorded on the Vacuum Generators UV-G3 spectrometer and calibrated with small amounts of Xe or Ar gas which was added to the sample flow. The spectral resolution in HeI and HeII spectra was 25 meV and 70 meV, respectively when measured as FWHM of the $3p^{-1}\ ^2P_{3/2}$ $Ar^+ \leftarrow Ar$ ($^1S_0$) line. The samples were recorded at temperatures 140–160 °C. The measured spectra were reproducible and showed no signs of decomposition.

The quantum chemical calculations were performed with GAUSSIAN 03 program [9a] including full geometry optimization of the neutral molecule at UB3LYP level as the first step. (The basis functions for all atoms were effective core potentials of SDD type [9b]). The eigenfunctions obtained via UDFT calculations were tested for stability in view of the paramagnetic nature of Gd and Yb complexes. KS orbital energies are known to be lower than the experimental vertical ionization energies, but their ordering provides correct sequence of ionic states for spectral assignment. This notion is confirmed in Table 1 where KS energies are in only a fair agreement with experimental values. The deficiency of such Koopmans type approximation can be circumvented by performing single point calculation with OVGF method [10]. The method obviates the need for Koopmans approximation and provides vertical ionization energies with typical deviation of 0.2–0.4 eV from the experimental value.

However, due to the size of our complexes we could not perform this calculation for the original complex species. We have instead performed OVGF calculations for the ligands themselves (acac, tmhd) (Table 1). We have also performed the OVGF calculation for tmhd negative anion, because tmhd ligands coordinating the metal atom have

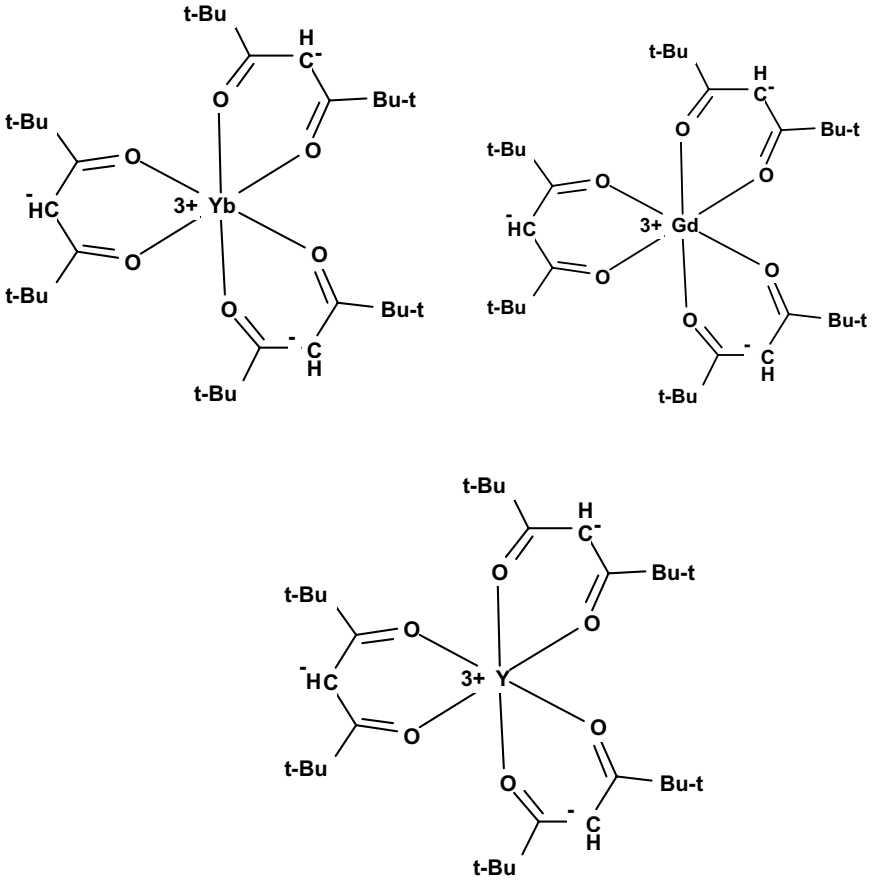

Scheme 1.

Table 1
Experimental (E_i/eV) and calculated (DFT–OVGF/eV) vertical ionization energies, assignments and relative band intensities of rare-earth β-diketonato complexes, their acetylacetone analogues, tmhd ligand and its anion

Complex	E_i	MO	Assignment	Rel. intensity	Acac analogues[a]
Y(tmhd)$_3$		*DFT*			*Y(acac)$_3$*
X	7.95	6.0	Y5s + π_{tmhd}	1 (HeI) 1 (HeII)	7.92
A–C	8.55	6.15, 6.45 6.61	π_{tmhd} n^-	1.63 (HeI) 1.7 (HeII)	8.20, 8.98
D–E	9.55	7.56, 7.70	n^-	1.24 (HeI) 1.10 (HeII)	9.14
	(10.8)				9.94, 10.26
Yb(tmhd)$_3$		*DFT*			*Yb(acac)$_3$*
X	8.05	6.0	Yb4f + π_{tmhd}	1 (HeI) 1 (HeII)	8.2
A–C	8.70	6.20, 6.42 6.64	π_{tmhd} n^-	1.9 (HeI) 0.64 (HeII)	8.2, 9.0
D–E	9.55	7.59, 7.73	n^-	1.34 (HeI) 0.55 (HeII)	9.0
	(10.05)				10.06, 10.3
Gd(tmhd)$_3$		*DFT*			*Gd(acac)$_3$*
X	7.8	6.12	Gd4f + π_{tmhd}	1 (HeI) 1 (HeII)	8.1
A–C	8.4	6.15, 6.42 6.64	π_{tmhd} n^-	2.0 (HeI) 0.83 (HeII)	8.1, 9.0
D–E	9.45	7.46, 7.64	n^-	1.6 (HeI) 0.63 (HeII)	9.0
	10.7				–
acac		*OVGF*			
X	9.18	9.07 (keto) 8.35 (enol)	n_- π		
A	9.74	9.62 (keto) 8.62 (enol)	n_+ n		
tmhd		*OVGF*			
X	8.65	8.47 (keto) 7.92 (enol)	n_- π	1 (HeI) 1 (HeII)	
A	9.1	9.07 (keto) 8.87 (enol)	n_+ n	1.4 (HeI) 1.3 (HeII)	
tmhd^{1-}		*OVGF*			
		7.30 9.3 9.95	π n_- n_+		

[a] Experimental data for acetylacetonates are from [5b].

negative charges. From such calculations we can establish the total number of ionizations below 10 eV, because the replacement of *t*-Bu with methyl groups in the ligand leads to only a small inductive shift in ionization energy. OVGF results indicate that one can expect six ionizations below 10 eV (Table 1).

The molecular structures of Y(tmhd)$_3$ and Gd(tmhd)$_3$ were determined by gas-phase electron diffraction and shown to have C_3 symmetry with the coordination sphere of metal resembling a distorted trigonal prism [11]. The calculated and experimental geometries are in good agreement with each other (Table 2). The complex molecule consists of three six member rings with each ring containing a metal atom and a bidentate tmhd ligand (Scheme 1). The rings are nonplanar with dihedral angles of 17° and 28° in Y(tmhd)$_3$ and Gd(tmhd)$_3$, respectively.

The nonplanarity suggests that steric crowding due to bulky *t*-Bu groups has important influence on the molecular structure and that the metal–ligand binding does not involve significant π-delocalization along the chelating ring. A further indication of relative weakness of the metal–ligand bond comes from the observed Y–O bond length of 2.23 Å which is very similar to Gd–O distance of 2.258 Å, even though the Y atom is much smaller than Gd. The bite angles in Y and Gd complexes are also similar at 75° and 72.8°, respectively.

3. Results and discussion

The HeI and HeII photoelectron spectra of rare-earth complexes and of the tmhd ligand are shown in Figs. 1–4. The spectral assignments are summarized in Table 1

Table 2
Estimated atomic valence orbital energies ε_i [13], photoionization cross-sections σ for atoms [12], calculated and observed geometrical parameters for Y and Gd complexes [11][a]

Atom	Orbital	ε_i (eV)	σ/Mb HeI/HeII	Geometrical parameters	Calc. (Å, °)	Obs. (Å, °)
Y	4d	6.22	4.8/0.51	Y–O	2.260	2.230
	5s	7.98	0.11/0.09	C–O	1.305	1.283
Gd	6s	6.15	0.09/0.075	C–C	1.408	1.411
	5d	7.37	4.71/0.80	≺OYO	73.7	75.0
	4f	9.29	0.5/1.287	≺CCC	124.3	123.7
Yb	6s	6.25	0.063/0.055			
	4f	7.77	1.19/2.42	Gd–O	2.254	2.258
Pd	4d	8.33	25.9/32.9	C–O	1.300	1.269
Pt	6s	8.96	0.02/0.03	C–C	1.410	1.391
	5d	9.72	29.4/31.3	≺OGdO	76	72.8
Co	4s	7.88	0.11/0.13	≺CCC	125	122.4
	3d	8.83	4.36/8.74			
V	4s	6.75	0.18/0.14			
	3d	7.35	5.80/5.93			
Cr	4s	6.76	0.06/0.05			
	3d	8.28	9.24/8.52			
Ni	4s	7.64	0.10/0.13			
	3d	7.81	3.97/8.42			
Cu	4s	7.73	0.04/0.04			
	3d	9.22	7.28/9.94			
Fe	4s	7.90	0.13/0.14			
	3d	9.29	4.83/8.75			

[a] The ground state electron configurations are: Y = [...]$4d5s^2$; Gd = [...]$4f^7 5d6s^2$; Yb = [...]$4f^{14}6s^2$.

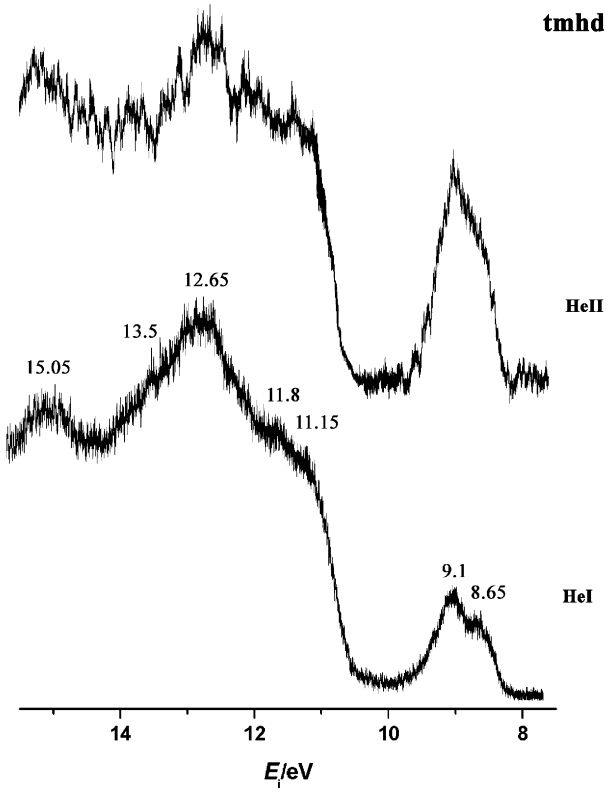

Fig. 1. HeI and HeII photoelectron spectra of the tmhd ligand.

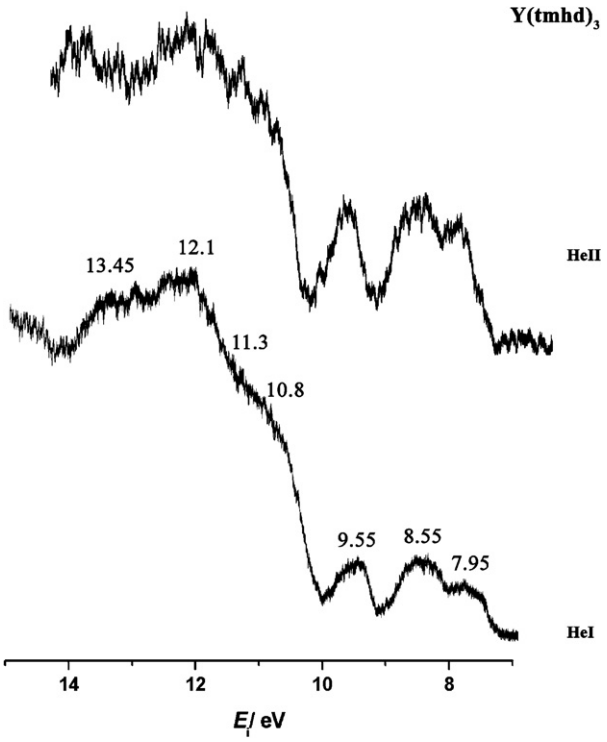

Fig. 2. HeI and HeII photoelectron spectra of the $Y(tmhd)_3$ complex.

together with UPS data on their acetylacetone analogues. Vovna et al. [5b] have performed measurements at single photon energy and used semi-empirical MO calculations for spectral analysis [5b]. Spectral measurements at more than one photon energy and higher level calculations are desirable to probe more reliably the details of ligand–metal bonding which was the purpose of this work. Comparison of ionization energies measured in [5b] and in this work

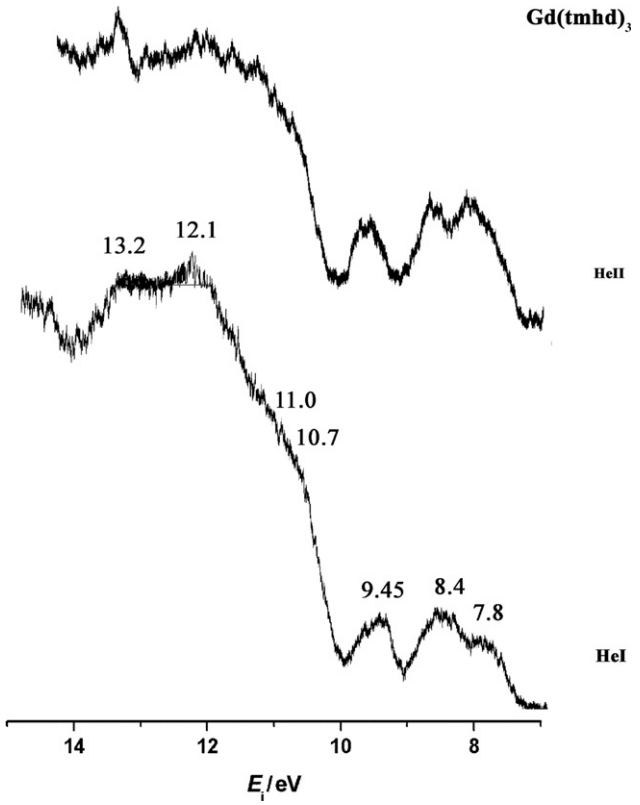

Fig. 3. HeI and HeII photoelectron spectra of the $Gd(tmhd)_3$ complex.

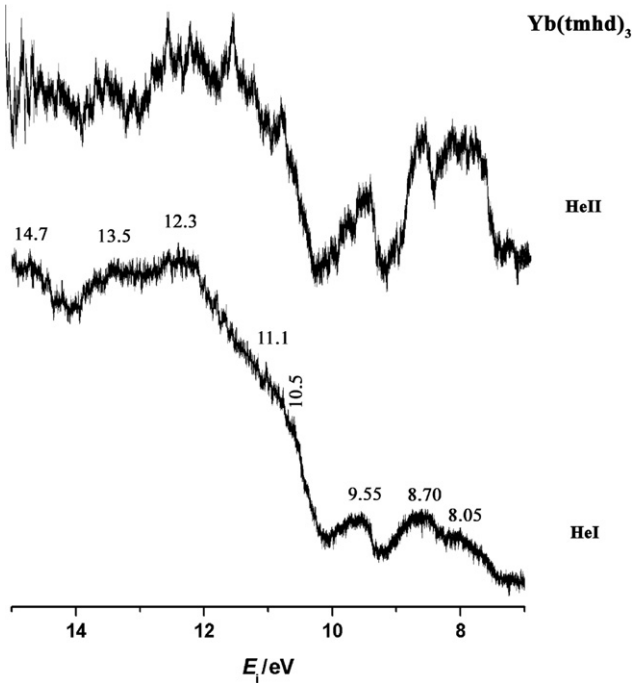

Fig. 4. HeI and HeII photoelectron spectra of the $Yb(tmhd)_3$ complex.

shows that rare-earth tmhd complexes have ionization energies which differ by 0.2–0.6 eV from their acac counterparts (Table 1). This shift in ionization energies can be attributed to the inductive effect of additional methyl groups present in tmhd complexes.

Due to the high density of ionic states above 10 eV, we confine our analysis to the bands whose ionization energies are below this value. The low molecular symmetry (C_3) allows many metal–ligand interactions to take place and lifts orbital degeneracies. This explains why even below 10 eV, the spectra contain three broad, partially resolved manifolds with relative intensity ratio 1:3:2. This high density of ionic states precludes accurate assignment of individual ionizations within the manifolds. We begin by recalling that acac and tmhd exist predominantly in enol form at the room temperature, while at higher temperatures (175 °C) the amounts of the two tautomers become nearly equal [1b]. UPS studies of acac ligand [1,4b] together with our OVGF calculations (Table 1) show that there are only two orbital ionizations below 10 eV (π and n_-). π is the antibonding orbital formed from the linear combination of two π_{CO} orbitals and the C2p orbital of central carbon [1]. n_+ and n_- designate symmetric and antisymmetric combinations of oxygen lone pairs, respectively. We have also measured the UPS of tmhd ligand (Fig. 1) which resembles the acac spectrum. The only difference between the spectra of the two ligands is the shift towards lower ionization energies in tmhd due to the inductive effect of *t*-Bu groups. The tmhd ligands in our complexes are in anionic form so we have performed the appropriate OVGF calculation for $tmhd^{1-}$ anion (Table 1). We obtained two ionizations for the anion which are significantly smaller than 10 eV and whose pole strengths are >0.92.

Since there are three tmhd ligands in each complex molecule, a total of six ligand orbital ionizations can be expected below 10 eV. However, some ligand orbitals may have metal character. UDFT results for the tmhd complexes and UPS spectra of rare-earth acac complexes [5b], also predict the total of six ionizations below 10 eV. The three partially resolved manifolds therefore correspond to ionizations from ligand (π_{tmhd}, n_-) and metal based orbitals (Y5s/4d, Gd6s/5d/4f, Yb6s/4f) (Fig. 5). In order to unravel the role of metal orbitals in bonding we measured the spectra at HeI and HeII photon energies. The HeI/HeII spectra of tmhd and acac ligands do not show changes in relative band intensities [4b, this work Fig. 1], so the HeI/HeII intensity changes observed in our spectra can be attributed to ionizations from the orbitals with metal character.

In the UPS of $Y(tmhd)_3$, $Gd(tmhd)_3$ and $Yb(tmhd)_3$we observed changes in relative HeI/HeII intensities of the first manifolds. This suggests that the first manifold contains ionizations from orbitals with metal character. In the spectra of $Y(tmhd)_3$ the change in the first manifold was less pronounced than in the other two complexes (Figs. 2–4). In order to understand this difference we consider the magnitudes of metal orbital photoionization cross-sections [12] and metal orbital energies. The latter values were estimated from atomic spectroscopy data [13]. The metal orbital energy was assumed to be equal to the average energy of

spectroscopic terms which are associated with the ground state electron configuration and weighted by the term degeneracies. We illustrate our procedure for deducing atomic orbital energies on the example of yttrium. The ground state electronic configuration of yttrium is $[\ldots]4d^15s^2$ and of Y^+ ion $[\ldots]5s^2$. Measured first ionization energy of yttrium is 6.22 eV so this value can be taken as an estimate of Y4d energy. Next we consider all spectroscopic terms with configuration $[\ldots]4d^25s^1$ and average their energies (weighted by respective angular momentum J multiplicities). The averaged energy, when added to 6.22 eV gives 7.98 eV which can be taken as an estimate of Y5s energy.

The metal photoionization cross-sections and orbital energies are given in Table 2. The photoionization cross-sections of Y5s, Gd6s, Yb6s orbitals vary little with photon energy, while Y4d and Gd5d cross-sections fall strongly on going from HeI to HeII. On the other hand, the cross-sections for Gd4f and Yb4f orbitals increase on going from HeI to HeII radiation (Table 2). The energy separations between ligand and metal orbitals are also important, because such separations (based on perturbation theory arguments) are a qualitative measure of orbital mixing/interactions; the smaller the separation, the better the mixing. In $Y(tmhd)_3$, $Gd(tmhd)_3$ and $Yb(tmhd)_3$ the energy separations between tmhd orbitals (8.65 eV) and Y5s, Gd4f and Yb4f orbitals are of similar magnitude and conducive to the metal–ligand interaction (Table 2). Y4d, Gd(5d+6s), Yb6s orbitals on the other hand, are further separated in energy from tmhd ligand orbitals and can be expected to make insignificant contribution to metal–ligand bonding. These arguments explain why is the intensity change in the first manifold of $Y(tmhd)_3$ smaller than in the other two rare-earth complexes. Taking into consideration the HeI/HeII intensity variations, relative band intensities of the three manifolds and the results of calculations, we arrived at the assignments given in Table 1.

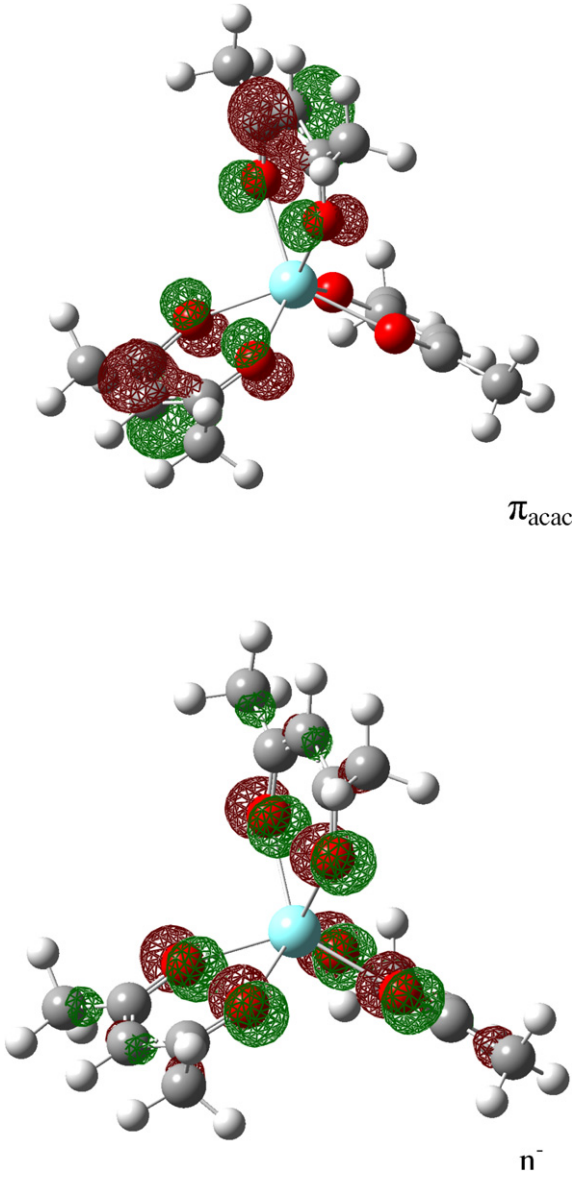

Fig. 5. Typical π and n_ orbitals in β-diketonato complexes.

Our conclusion is that metal orbitals play a significant role in metal–ligand bonding of all three complexes. However, this conclusion does not follow directly from the corresponding HeI/HeII intensity variations. Indeed, the intensity changes alone would suggest that in $Gd(tmhd)_3$ and $Yb(tmhd)_3$, metal orbitals participate more in the metal–ligand bonding than they do in $Y(tmhd)_3$. However, after photoionization cross-sections are included in the analysis we suggest that all three metals have comparable metal–ligand interactions.

We extend our analysis to the previously reported HeI/HeII spectra of three sets of metal β-diketonato complexes. The first set comprises UPS of Pd and Pt complexes [4c]. The 4th and 3rd bands in the UPS of Pd and Pt complexes, respectively show considerable intensity enhancement on going from HeI to HeII. The enhancements can be attributed to Pd4d and Pt5d characters of the respective orbitals. The intensity change is more pronounced in the Pd complex than in its Pt analogue [4c] even though the Pt5d energy is closer to acac orbital energies than is Pd4d (Table 2). This can be rationalized by noting that Pd4d cross-section varies more than Pt5d on going from HeI to HeII radiation. We thus suggest that Pd participates more strongly in metal–ligand bonding than Pt. This conclusion was derived on the basis of empirical arguments rather than via quantum chemical calculations.

The second set comprises the HeI/HeII spectra of $Co(acac)_3$, $V(acac)_3$ and $Cr(acac)_3$. The first band in each spectrum shows an enhancement in relative intensity (on going from HeI to HeII) and was therefore attributed to orbital with metal 3d character [3]. However, the intensity enhancement is strongest in Co and weakest in V complex. We suggest that this is due to Co3d energy being closest to the energy of acac orbitals and also because Co3d photoionization cross-section increases on going from HeI to HeII radiation. On the other hand, V3d energy is not well matched to acac orbitals and V3d cross-section does not

vary much at HeI/HeII energies (Table 2). Cr3d orbital is an intermediate case: good energy match to ligand orbitals, but slight decrease in photoionization cross-section. The first UPS band of $Cr(acac)_3$ thus exhibits only a small intensity change.

The third set of HeI/HeII spectra consists of $Ni(acac)_2$ and $Cu(acac)_2$ complexes. Modest intensity enhancements of the 3rd and the 4th band were detected in Ni and Cu complexes [4b]. Inspection of Table 2 suggests the explanation for this observation. Ni3d energy does not match ligand orbital energies well, but its cross-section is enhanced twofold on going from HeI to HeII. On the other hand, Cu3d matches ligand energy levels well, but its cross-section increases by only 25% in the same photon energy range.

4. Conclusion

We reinvestigated the role of metal orbitals in metal–ligand bonding of β-diketonato complexes. The extent of metal participation in bonding cannot be reliably ascertained through quantum chemical calculations or relative band intensity changes (at various photon energies) alone. The rationalization of metal–ligand bonding requires consideration of metal orbital energies as well as their photoionization cross-sections. This had so far been done in only a few instances and we provide a cautionary example which illustrates various factors influencing UPS band intensities of the title complexes.

References

[1] (a) S. Evans, A. Hamnett, A.F. Orchard, D.R. Lloyd, Faraday Discuss. Chem. Soc. 54 (1972) 227;
(b) A. Schweig, H. Vermeer, U. Weidner, Chem. Phys. Lett. 26 (1974) 229.
[2] H.G. Brittain, R.L. Disch, J. Electron Spectrosc. Relat. Phenom. 7 (1975) 475.
[3] H. van Dam, A.D. Oskam, J. Electron Spectrosc. Relat. Phenom. 17 (1979) 353.
[4] (a) C. Cauletti, M. de Simone, S. Stranges, M.N. Piancastelli, M.-Y. Adam, F. Cirilli, A. Ianninello, J. Electron Spectrosc. Relat. Phenom. 76 (1995) 277;
(b) C. Cauletti, C. Furlani, G. Storto, J. Electron Spectrosc. Relat. Phenom. 18 (1980) 329;
(c) S. di Bella, I. Fragala, G. Granozzi, Inorg. Chem. 25 (1986) 3997.
[5] (a) A.Yu. Ustinov, V.I. Vovna, O.M. Ustinova, J. Electron Spectrosc. Relat. Phenom. 88–91 (1998) 103;
(b) V.I. Vovna, V.V. Gorchakov, A.I. Cherednichenko, N.G. Dzhyubenko, N.P. Kuzmina, L.I. Martynenko, Koord. Khim. 17 (1991) 571.
[6] V.I. Vovna, I.S. Osmushko, J. Struct. Chem. 45 (2004) 617.
[7] J. Selbin, N. Ahmad, N. Bhacca, Inorg. Chem. 10 (1971) 1383.
[8] G. Richer, C. Sandorfy, J. Mol. Struct. (Theochem) 167 (1988) 413.
[9] (a) M.J. Frisch, G.W. Trucks, H.B. Schlegel, G.E. Scuseria, M.A. Robb, J.R. Cheeseman, V.G. Zakrzewski, J.A. Montgomery Jr., R.E. Stratmann, J.C. Burant, S. Dapprich, J.M. Millam, A.D. Daniels, K.N. Kudin, M.C. Strain, O. Farkas, J. Tomasi, V. Barone, M. Cossi, R. Cammi, B. Mennucci, C. Pomelli, C. Adamo, S. Clifford, J. Ochterski, G.A. Petersson, P.Y. Ayala, Q. Cui, K. Morokuma, D.K. Malick, A.D. Rabuck, K. Raghavachari, J.B. Foresman, J. Cioslowski, J.V. Ortiz, B.B. Stefanov, G. Liu, A. Liashenko, P. Piskorz, I. Komaromi, R. Gomperts, R.L. Martin, D.J. Fox, T. Keith, M.A. Al-Laham, C.Y. Peng, A. Nanayakkara, C. Gonzalez, M. Challacombe, P.M.W. Gill, B. Johnson, W. Chen, M.W. Wong, J.L. Andres, C. Gonzalez, M. Head-Gordon, E.S. Replogle, J.A. Pople, GAUSSIAN 03, Revision D1, Gaussian, Inc., Pittsburgh, PA, 2003;
(b) A. Bergner, M. Dolg, W. Kuechle, H. Stoll, H. Preuss, Mol. Phys. 80 (1993) 1431.
[10] W. Von Niessen, J. Schirmer, L.S. Cederbaum, Comp. Phys. Rep. 1 (1984) 57.
[11] (a) S. Shibata, K. Iijima, T. Inuzuka, J. Mol. Struct. 144 (1986) 181;
(b) S. Shibata, K. Iijima, T. Inuzuka, S. Kimura, T. Sato, J. Mol. Struct. 144 (1986) 351.
[12] J.J. Yeh, Atomic Calculation of Photoionization Cross-sections and Asymmetry Parameters, Gordon and Breach, Langhorne, 1993.
[13] J.E. Sansonetti, W.C. Martin, J. Phys. Chem. Ref. Data 34 (2005) 1559.